Eruptive proceses responsible for fall tephra in the Upper Miocene Peralta Tuff, Jemez Mountains, New Mexico

Sharon Kundel and Gary A. Smith

2007, pp. 268-274. https://doi.org/10.56577/FFC-58.268

in:

Geology of the Jemez Region II, Kues, Barry S., Kelley, Shari A., Lueth, Virgil W.; [eds.], New Mexico Geological Society 58 th Annual Fall Field Conference Guidebook, 499 p. https://doi.org/10.56577/FFC-58

This page is intentionally left blank to maintain order of facing pages.

New Mexico Geological Society Guidebook, 58th Field Conference, Geology of the Jemez Mountains Region II, 2007, p. 268-274.

ERUPTIVE PROCESSES RESPONSIBLE FOR FALL TEPHRA IN THE UPPER MIOCENE PERALTA TUFF, JEMEZ MOUNTAINS, NEW MEXICO

SHARON KINDEL AND GARY A. SMITH
Department of Earth and Planetary Sciences, MSC03 2040, University of New Mexico, Albuquerque, NM, 87131-0001; ssparks@unm.edu

ABSTRACT — Upper Miocene pyroclastic-fall deposits in the southeastern Jemez Mountains consist of of a distinct tripartite stratigraphy. A lower white interval is a thick (~0.5-3.0 m), massive, moderately sorted, coarse-grained, pumice-lapilli layer, with abundant, non-glassy lithic fragments. A central pink interval is a much thinner (~8-12 cm), moderately sorted, laminated fine ash with few dispersed coarser fragments. A top gray interval (~15 cm-1.1 m) is stratified and composed of well-sorted, poorly vesicular perlite fragments. At least eight pyroclastic-fall deposits contain this stratigraphy, suggesting a repetitive process of changing eruption dynamics that was common to several different eruptions. Detailed study of two deposits implies a three-stage eruptive history. White intervals were produced by explosive plinian or subplinian eruptions of gas-rich magma. The pink intervals were deposited from coignimbrite ash clouds, and one pink layer is traceable laterally into a pyroclastic-flow deposit. The gray intervals resulted from fragmentation and rapid decompression of highly viscous, partly solidified magma high in the conduit as a consequence of surface dome collapse. This latter stage of activity may have been intermittent and coeval with a long period of dome growth, as suggested by minor erosional disconformities within gray-interval tephra.

INTRODUCTION

Pyroclastic-fall deposits reveal information about eruption style, pyroclast transport and deposition processes, fragmentation processes, and eruption-column characteristics (e.g., Carey and Sparks, 1986; Carey and Sigurdsson, 1987; Cas and Wright, 1987; Houghton and Wilson, 1989; Klug and Cashman, 1996; Wilson and Hildreth, 1997). Most studies of stratigraphic variability within fall tephra focus on pumiceous deposits from plinian columns, which likely accumulated over a matter of hours to a few days. This paper focuses on decimeter- to meter- scale stratification of particle types that reveal temporal variation in eruption dynamics over longer time intervals, perhaps months to years.

We describe and interpret upper Miocene rhyolitic pyroclastic-fall deposits in the southeastern Jemez Mountains, New Mexico, that contain three distinct horizons. In each deposit, the lowest horizon is a ~0.5-3.0 m-thick layer of white, stratified to massive pumice lapilli and minor ash. The middle pink layer is a much thinner (~8-12 cm), moderately sorted, laminated fine ash with minor dispersed coarser fragments. The upper gray layer (~15 cm-1.1 m) is stratified, and composed of well-sorted, poorly vesiculated perlite fragments. At least eight pyroclastic-fall deposits in the study area exhibit this stratigraphy, suggesting a repetitive process of changing eruption dynamics that was common to many different eruptions.

We hypothesize a three-stage eruption history to account for this stratification. The first eruptive stage, producing the lower white layer, is fallout of pumice lapilli and lithic fragments from steady, plinian, or pulsating subplinian, eruption columns. The second stage, producing the pink layer, involved ash-cloud deposition from pyroclastic flows. Lastly, the gray layer resulted from explosions ejecting partially to largely degassed magma.

The dynamics of pyroclastic eruptions can be interpreted by consideration of fragment grain size, texture, composition, and vesicularity. The purpose of this study is to use these characteristics to test the stated hypothesis and to reconstruct the volcanic processes responsible for two deposits in the Jemez Mountains study area.

STUDY AREA

The study area is located in the southeastern Jemez Mountains in north-central New Mexico, along the western margin of the Rio Grande rift (Fig. 1). The Jemez Mountains volcanic field is best known for highly explosive, early Pleistocene eruptions that produced the Bandelier Tuff and the Valles caldera (Smith and Bailey, 1966; Smith et al., 1970). However, volcanism in the field commenced no later than 16 Ma, producing middle and upper Miocene volcanic rocks of the Keres Group, which are predominant in the southern Jemez Mountains. Andesite, basalt, and dacite of the Paliza Canyon Formation form the bulk of the Keres Group, and the Bearhead Rhyolite forms the uppermost part of the Keres Group (Gardner et al., 1986). The Bearhead Rhyolite consists of numerous small-volume, sparsely phyric (<5% phenocrysts), high-silica (~75 wt. % SiO_2) rhyolitic domes, plugs, and flows, as well as related pyroclastic deposits that originated from lower-crust melts and were erupted along Rio Grande rift-related faults (Ellisor et al., 1996; Smith, 2001; Justet and Spell, 2001).

The Peralta Tuff Member of the Bearhead Rhyolite consists of high-silica rhyolite pyroclastic deposits resulting from pyroclastic falls, flows, and surges. These deposits are locally interbedded with fluvial and eolian sedimentary facies and have total thicknesses of at least 500 m. More than 40 eruptions from at least 20 vents occurred between ~7.06 and 6.15 Ma (Smith, 2001).

The stratigraphy of the Peralta Tuff Member is well exposed and well known in the Colle Canyon-Peralta Canyon area (Figs. 1, 2), where primary-pyroclastic and sedimentary facies accumulated within a subsiding rift basin (Smith, 2001). At least eight fall deposits exhibit the tripartite stratigraphy of interest to

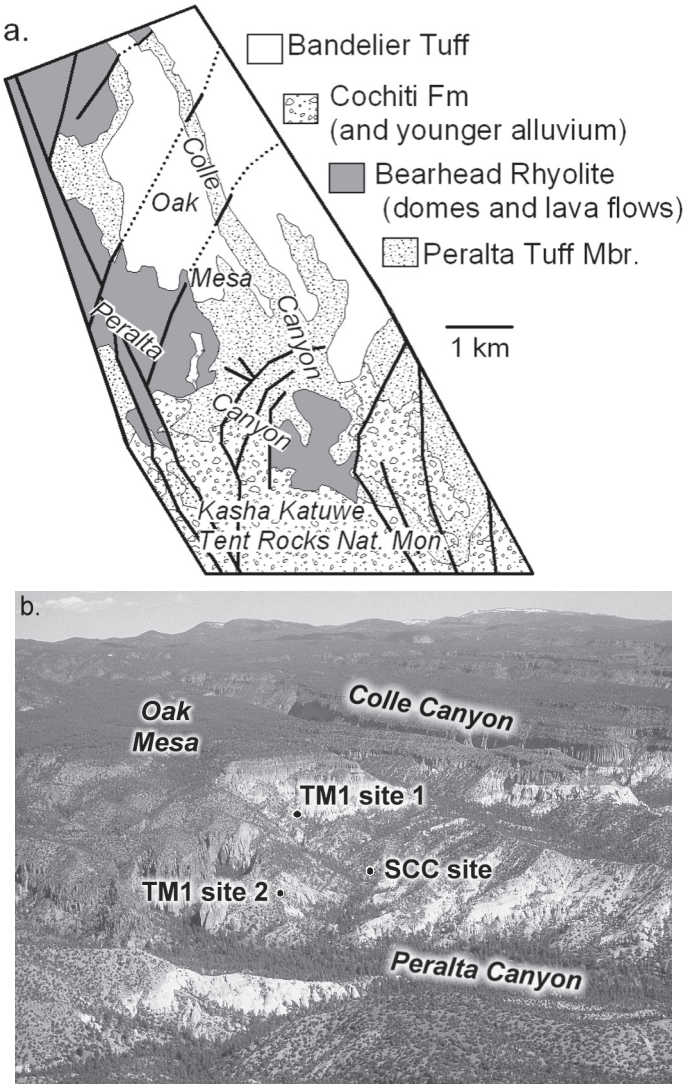

FIGURE 1. **a.** Geologic map (after Smith, 2001) of the study area. **b.** Olique-aerial photograph showing the location of sites 1 and 2 (Tephra Marker 1) and site 3 (Sub-Colle Canyon Tephra). The distance between each site is ~600-700 m.

this study. Two of the thickest and most widely exposed deposits were chosen for closer study. None of these upper Miocene deposits are exposed over sufficiently broad areas to permit study of regional variations in grain size that would permit estimation of column heights and discharges (cf. Carey and Sparks, 1986). As a result, our investigation focused on one, well-exposed and reasonably complete stratigraphic section through each of the two deposits (Fig. 1) and cursory observations at nearby outcrops. The two fall deposits (Figs. 2, 3) are informally named tephra-marker 1 (TM1) and the sub-Colle Canyon tephra (SCC). The SCC tephra, which is subjacent to pyroclastic-flow deposits of the tuff of Colle Canyon (Fig. 2), is locally separated from the flow deposits by a paleosol. The paleosol indicates that the SCC tephra and tuff of Colle Canyon formed during different eruptive events. It is not possible to determine the source vent for either tephra, but five Bearhead Rhyolite dome and intrusive complexes are present within a 6-km radius of the studied outcrops.

RESEARCH METHODS

Field descriptions and stratigraphic sections were completed at one outcrop of each tephra. Physical properties of each texturally distinct layer were described using a sedimentological

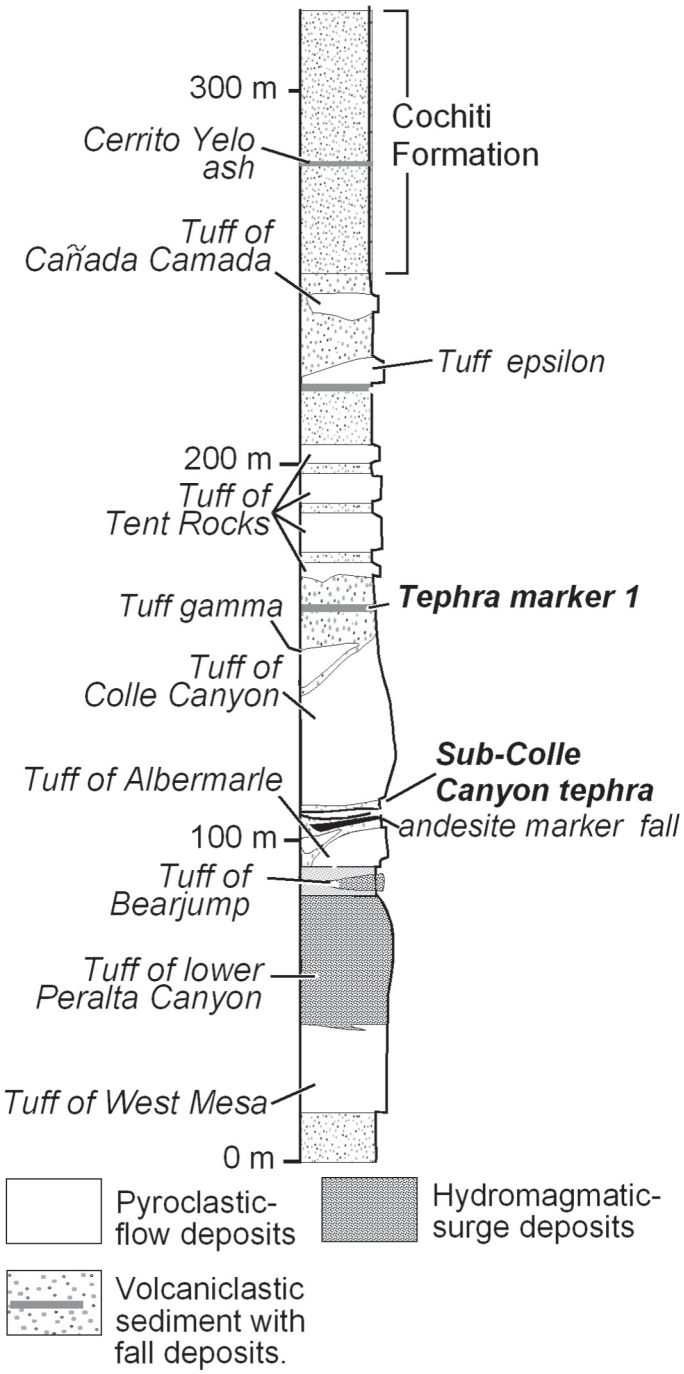

FIGURE 2. Generalized stratigraphy of the Peralta Tuff Member of the Bearhead Rhyolite in the Colle Canyon-Peralta Canyon-Tent Rocks area. The stratigraphic position of Tephra Marker 1 and the Sub-Colle Canyon tephra are shown, (after Smith, 2001).

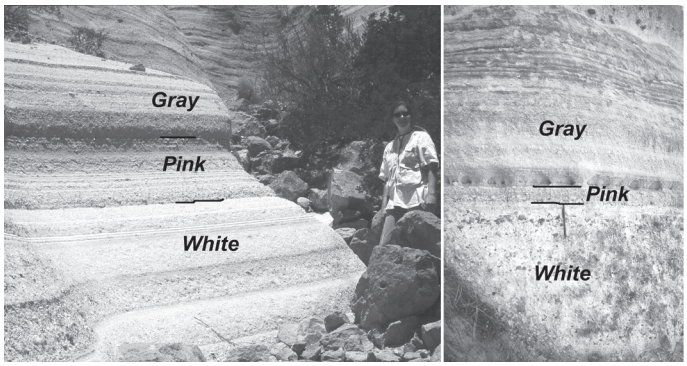

FIGURE 3. Outcrop photographs of Tephra Marker 1 at site 1 (left) and the Sub-Colle Canyon tephra fall deposit at site 3 (right), both showing the following complex stratification: a lower white interval composed of coarse, interlayered-pumice lapilli with minor ash; an intermediate pink interval composed of fine ash and lapilli; and an upper gray interval composed of perlite-rock fragments.

approach, and included records of total thickness of each layer, estimated average grain size, largest pumice fragment, estimated average pumice size, largest lithic fragment, estimated average lithic size, and estimated percentage of pumice and lithic fragments. In addition, samples were collected for laboratory studies as described below.

Grain-size analyses of samples from white and gray intervals were performed with sieves following the methods of Folk (1974) and Lewis and McConchie (1994). Disaggregated samples of white and gray layers were mechanically sieved in ½ ϕ intervals between –3.0 ϕ and 4.0 ϕ. No grain-size data were collected for the pink intervals because of cementation that precluded disaggregation.

Component analyses of grains from the white and gray layers were performed with a binocular microscope. 100 grains in the -1.5ϕ to –3.0ϕ size classes were point-counted to obtain percentages of pumice and vesicular perlite, dense perlite, devitrified rhyolite, andesite, and hydrothermally altered volcanic rock fragments. Juvenile glassy components range gradationally from slightly vesicular perlite to highly vesicular pumice, especially in the gray layers. For objective consistency, visibly vesicular perlite and pumice were counted in one category.

Petrographic and scanning electron microscope (SEM) observations were made of selected samples, primarily to examine fragment vesicularity. Selected polished thin sections were examined in a JEOL® JSM-5800 LV SEM. In addition, 0.0Φ-sieve-fraction particles from two gray-interval and two white-interval samples were examined in the SEM. The volume fraction of bubble surface on glassy-pyroclastic fragments was estimated by visual comparison to images of particles of known vesicularity illustrated in Marshall and Sheridan (1987). Fifty-three SEM images were used to describe the fraction of bubble surface in intervals of 0.1 (i.e. 10%). Multiple analyses by both authors were compared and found to be highly consistent between analyses by each worker and between workers with reproducibility within 0.1.

RESULTS

The white interval

The TM1 white interval shares many similarities with the white interval within the SCC tephra. The white intervals at both sites are composed of poorly sorted, coarse-grained, highly vesicular pumice lapilli (Fig. 4) with generally more than 20% accessory-lithic fragments (Table 1). The two white intervals contain similar dominant abundances of pumice, and a diverse assemblage of lithic fragments that includes numerous hydrothermally altered fragments and clasts of the underlying Paliza Canyon Formation andesite (Table 1). In addition, many of the lithic fragments are as coarse (and coarser) than the pumice fragments (Fig. 4). This

Table 1. Composition of –1.5 to 3.0 ϕ size class of selected layers

			% Juvenile fragments		% Accessory lithic fragments			
Tephra	**Layer (color)**	**Total fragments counted**	**Pumice & vesicular perlite**	**Dense perlite**	**devitrified rhyolite**	**andesite**	**Hydrothermally altered volcanic rocks**	**Total % accessory lithic fragments**
TM1	L-9 (white)	745	66.7	0.9	16.8	2.5	13.0	32.4
TM1	L-10 (white)	546	83.9	2.6	9.5	0.5	3.5	13.6
TM1	L-12 (white)	599	73.6	4.7	14.2	3.2	4.3	21.7
SCC	L-1 (white)	691	77.3	0.7	10.0	0.9	11.1	22.0
	Avg. (white)	*2581*	*74.8*	*2.1*	*12.8*	*1.8*	*8.5*	*23.1*
TM1	L-23 (gray)	522	43.7	19.2	26.6	1.5	9.0	37.2
TM1	L-24 (gray)	511	55.8	29.0	11.4	0.0	3.9	15.3
TM1	L-25 (gray)	439	62.9	27.3	5.9	0.2	3.6	9.8
SCC	L-12 (gray)	319	52.4	36.1	6.3	0.0	5.3	11.6
SCC	L-14 (gray)	528	43.2	30.3	24.2	0.4	1.9	26.5
SCC	L-22 (gray)	261	35.3	59.0	3.1	0.4	2.3	5.8
	Avg (gray)	*2580*	*49.5*	*30.9*	*14.7*	*0.5*	*4.5*	*19.6*

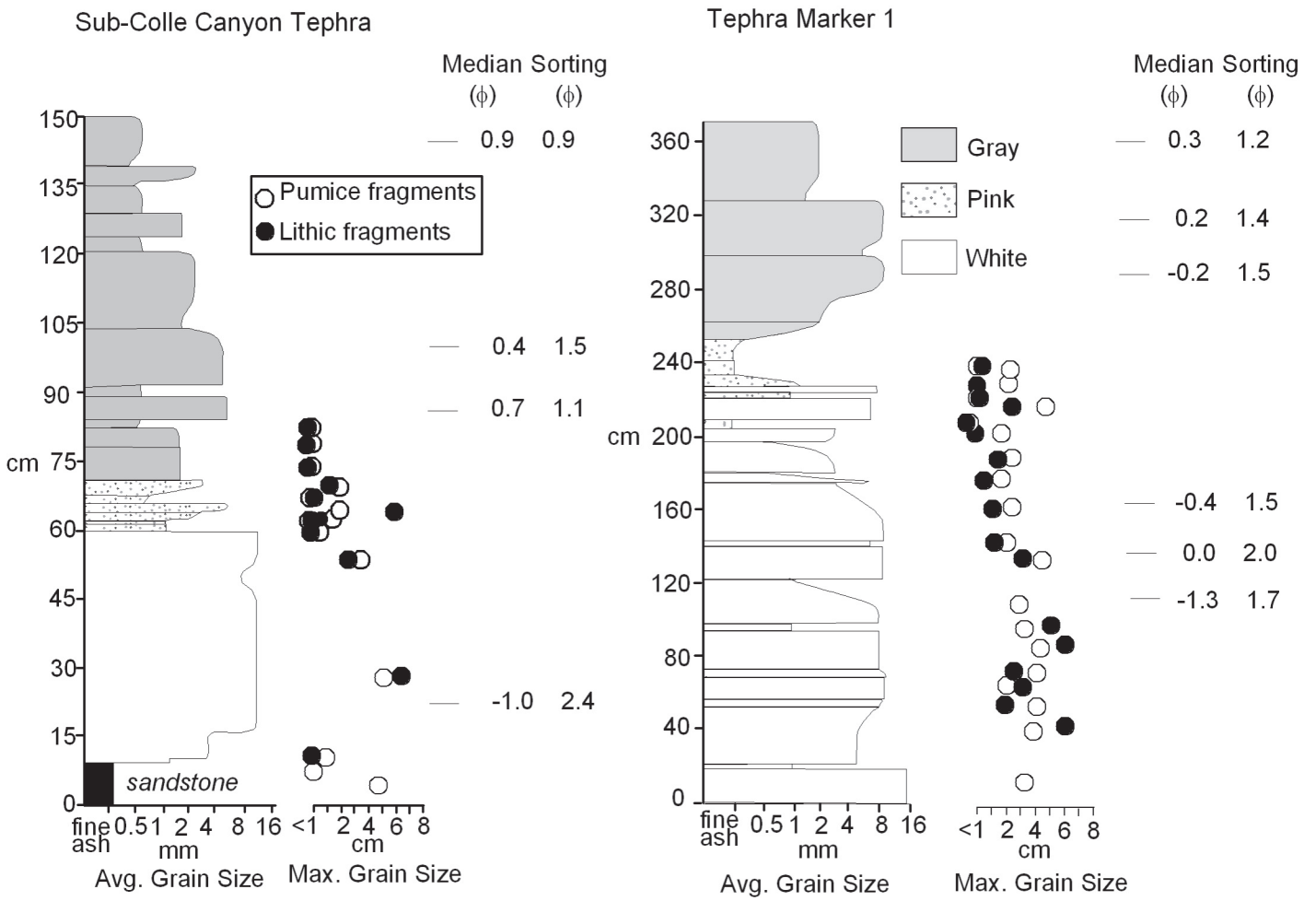

FIGURE 4. Stratigraphic columns of the Sub-Colle Canyon tephra at site 3 (left) and TM1 at site 1 (right), with maximum grain size plots and median/sorting values (plotted next to layers that were sieved). There are no maximum pumice or lithic-clast data for the gray intervals because these layers consist of abundant perlite fragments of varying vesicularity that are not objectively distinguished as pumice or dense lithic fragments in the field.

phenomenon is in contrast to the observation that dense-lithic fragments are usually smaller than adjacent vesicular pumice (e.g., Cas and Wright, 1987).

The white intervals at both sites differ significantly in thickness and stratification (Figs. 3, 4). The ≈2.0 m-thick white interval in TM1 at site 1 is internally stratified and contains coarser grain sizes near the base, with an abrupt grain-size decrease that occurs higher up in the deposit (Fig. 3). Some thin, pink-ash laminae are present between white-pumice lapilli and ash layers in the upper part of TM1 (Fig. 3). The ≈0.5 m-thick white interval from the SCC tephra at site 3 lacks stratification but does exhibit very subtle grain-size variations and an inversely graded base (Fig. 3).

The pink interval

The pink intervals in TM1 and the SCC tephra consist of poorly to moderately sorted, laminated fine ash with minor dispersed coarser pumice fragments. In contrast to the unconsolidated nature of the white and gray intervals, the pink intervals are cemented by silica and clay. Coarse pumice lapilli are sparse in the lower parts of the pink intervals, and are completely absent in the upper parts. The ≈0.2 m-thick pink interval in TM1 is internally plane stratified, whereas no stratification is apparent in the thinner (≈0.1 m) pink interval in SCC.

We traced the middle pink ash in TM1 for ≈670 m into a 30 cm-thick pyroclastic flow deposit (Fig. 6). Therefore the pink layer in the fall deposit is the lateral equivalent of the pyroclastic-flow deposit.

The gray interval

The gray intervals in both tephra portray similarities and differences. In both cases, the tops of the deposits are eroded, so the original thicknesses of the gray intervals are not known. The ≈1.0 m-thick gray interval in TM1, and the ≈0.8 m-thick gray interval in the SCC tephra are both composed of fine- to medium-grained, well-sorted (Fig. 4) variably vesicular to dense perlite (originally obsidian) fragments (Fig. 7). The gray intervals contain vesicular fragments (Table 1), but the vesicularity of the majority of the fragments is low compared to the pumice lapilli in the white intervals (compare Figs. 5 and 7). The gray intervals are inter-

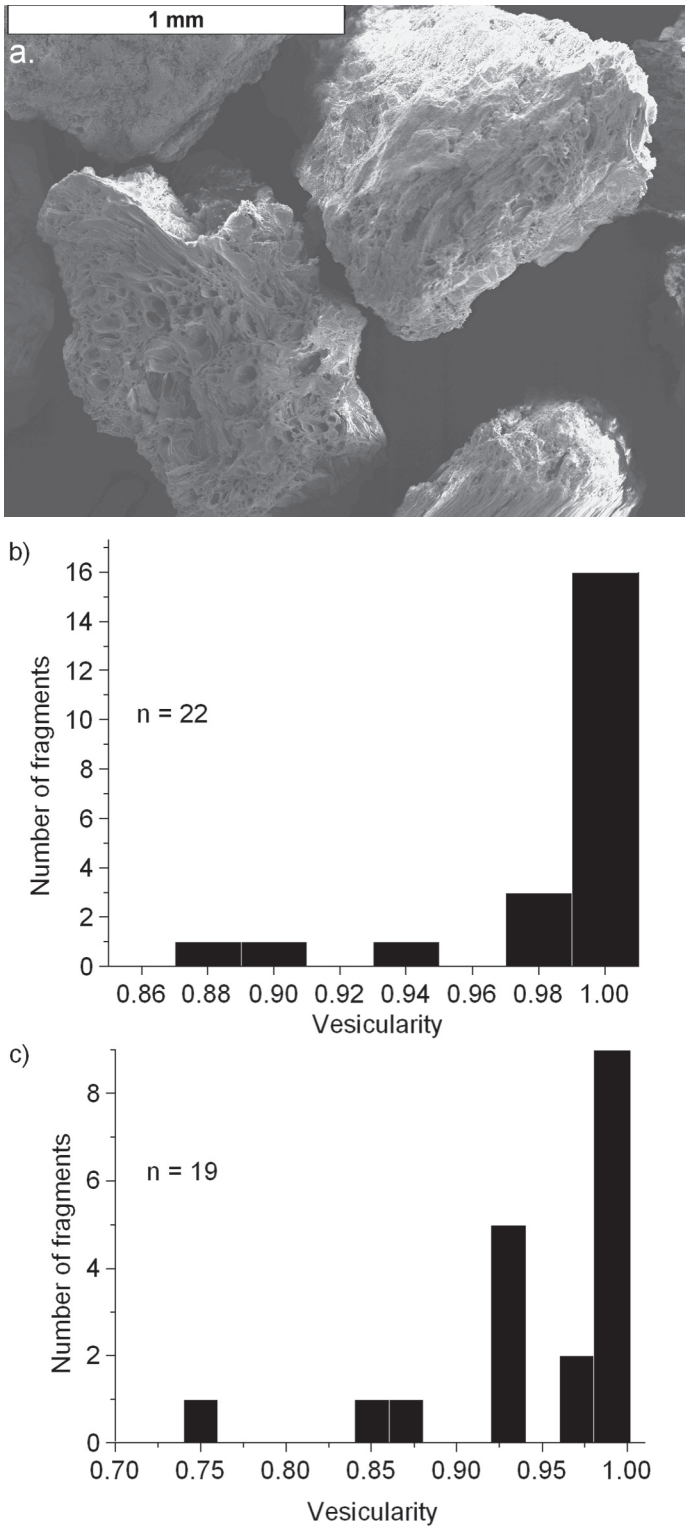

FIGURE 5. **a.** SEM image of vesicular-pumice pyroclasts from the white interval in the SCC tephra. These clasts were assigned an average vesicularity value of 0.9. **b.** Histogram of pumice-vesicularity data from the white interval in the SCC tephra at site 3. **c.** Histogram of pumice-vesicularity data from the white interval in TM1 at site 1.

nally stratified at both sites (Fig. 3). Low-angle erosional surfaces are also present, implying hiatuses during accumulation.

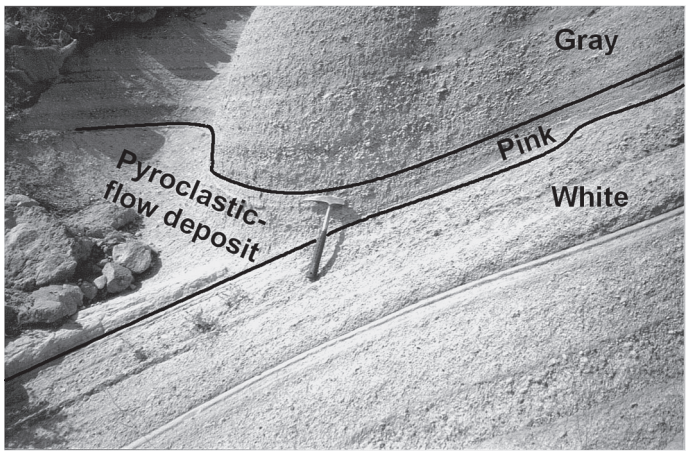

FIGURE 6. Outcrop photograph of a 30 cm-thick pyroclastic flow deposit (site 2) that is transitional to the pink interval in TM1.

The accessory lithic fragment content of the gray intervals is generally lower than in the white intervals. Nonglassy, nonjuvenile lithic fragments are mostly devitrified rhyolite and there are notably fewer hydrothermally altered and older andesite fragments compared to the white intervals (Table 1).

DISCUSSION

Eruption processes responsible for the white intervals

The white intervals from both sites are dominated by coarse, highly vesicular pumice, accompanied by a diverse suite of coarse lithic fragments (Figs. 4, 5; Table 1). Therefore, these intervals were produced by explosive eruptions of volatile-rich magma with fragmentation processes that were driven by the expansion and bursting of bubbles. The presence of a diverse suite of lithic fragments, including the abundance of hydrothermally altered fragments (Table 1) indicates vent-widening processes and likely derivation of clasts over a broad depth range, including the hydrothermal regime adjacent to the Bearhead Rhyolite intrusions.

The observation that maximum-sized lithic fragments within the white intervals of both deposits are as coarse (or coarser) than the pumice fragments (Fig. 4) is puzzling. We speculate that the larger lithic fragments may be of ballistic origin rather than dispersed from a convective tephra plume. Given the proximity of possible vent sites within 2 to 6 km, it is reasonable to expect the presence of ballistic projectiles.

Stratification and abrupt grain-size changes in the white interval of TM1 (Figs. 3, 4) record a less steady magma flux and a more variable eruption column than for the SCC-tephra eruption. The SCC tephra has characteristics of plinian eruptions whereas the TM1 fall may have been produced by a subplinian eruption (e.g., Cas and Wright, 1987). These characteristics are consistent with a plinian eruption for the deposition of the SCC white interval and a subplinian eruption for TM1. In addition, generally coarser grain sizes near the base of TM1 suggest that the flux and column height were greatest during the early stages of the eruption. Lastly, the presence of some thin pink-ash laminae between white-pumice lapilli and ash layers in the upper part of the TM1

white interval at site 1 (Fig. 4), suggest a gradual transition to processes responsible for depositing the pink interval.

Eruption processes responsible for the pink intervals

The coloration and poor to moderate sorting of the pink intervals, in addition to the correlation of the TM1 pink interval to a pyroclastic-flow deposit (Fig. 6), are all consistent with an origin related to coignimbrite ash clouds (e.g., Cas and Wright, 1987). The distinctive pink coloration is probably due to thermal oxidation of finely disseminated magnetite in glass shards while the co-ignimbrite ash clouds were suspended.

Larger dispersed fragments within the pink intervals can be interpreted to be from either lapilli entrained in ash clouds or the contemporaneous fallout of fragments from an eruption column. However, the scarcity of coarse pumice lapilli in these intervals and their absence in the uppermost part of these pink intervals, suggest that pyroclastic-flow emplacement followed, but was not accompanied by, a high-standing convective eruption column. The restricted nature of the pink intervals within the fall-deposit stratigraphy suggests that pyroclastic flows were emplaced during a relatively narrow time window in the overall eruption history.

Eruption dynamics responsible for the gray intervals

The high abundance of perlite (originally obsidian), angular, blocky shapes of the fragments (Fig. 7a), and low degree of vesiculation (Fig. 7b) in the gray intervals are consistent with fragmentation by decompression of highly viscous rhyolite, either high in the conduit (cryptodome) or extruded as a lava dome (cf. Alidibirov and Dingwell, 2000). The low abundance of deeply derived andesitic and hydrothermally altered fragments suggests that most of the explosions originated high in the conduit. The internal stratification implies a pulsating eruption column, or many discrete explosions with eruptive hiatuses that are also suggested by the presence of low-angle erosional surfaces.

The volatile pressure to produce these explosions may have resulted from one of four different mechanisms: (1) new volatile-rich magma may have risen high into the conduit; (2) magma at depth may have partially crystallized anhydrous phases, causing volatile pressure to increase; (3) external meteoric water may have been introduced and triggered phreatic or phreatomagmatic explosions; and (4) dome collapse may have decompressed the magma within the conduit and deeper within the dome to trigger explosions.

The first scenario seems unlikely, because it should result in a mixture of vesicular pumice (from the newly introduced magma) along with the dense obsidian fragments; pumice lapilli are, however, rare to absent in the gray layers. The second mechanism also seems unlikely, because of the extremely low phenocryst content (<5%) of most Bearhead Rhyolite lava and intrusions. If high-level phreatic or phreatomagmatic explosions had fragmented a cooling dome, as proposed in the third mechanism, we would expect a large proportion of fine, highly fragmented ash, rather than the coarse ash and lapilli that form the gray intervals. We find the characteristics of the gray intervals to be most consistent with fragmentation of highly viscous magma by rapid decompression as outlined by Alidibirov and Dingwell (2000). Rapid pressure release that caused progressive downward decompression, fragmentation, and explosive ejection of the cooling magma is most readily attributed to dome collapse at the surface.

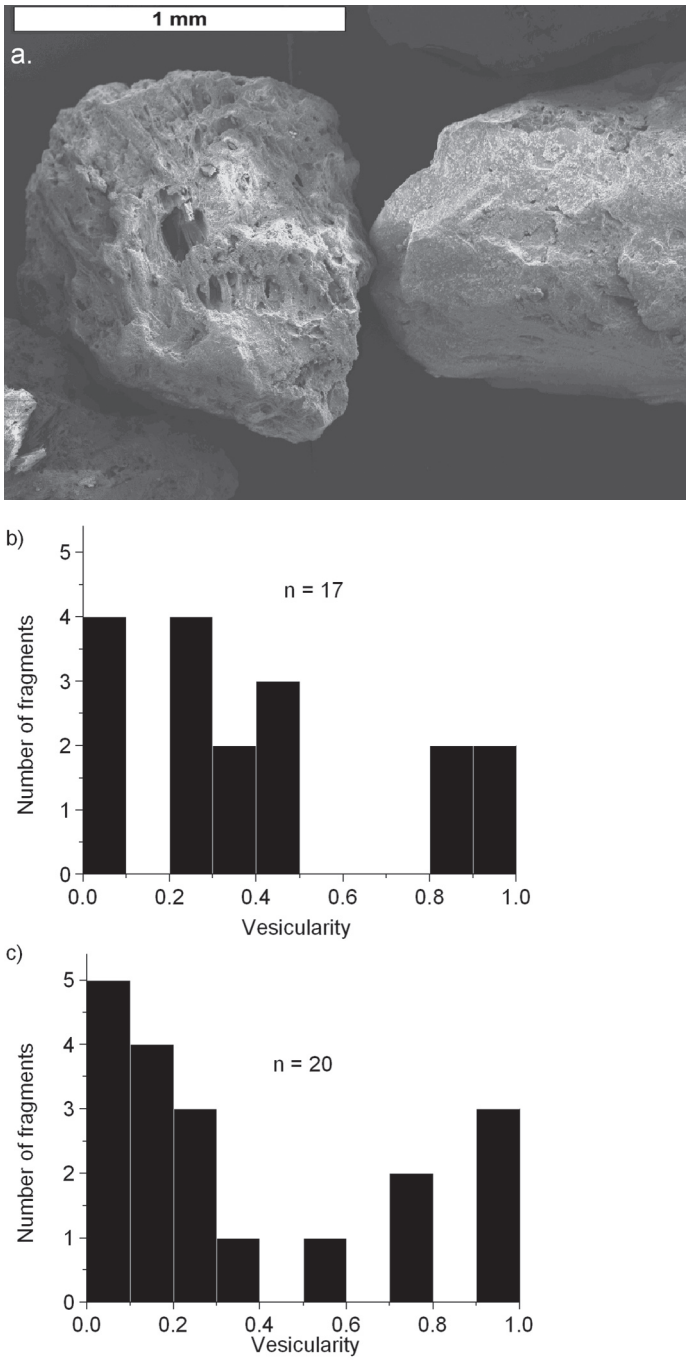

FIGURE 7. **a.** SEM image of dense-perlite fragments from the gray interval in TM1. These clasts were assigned an average vesicularity value of 0.8 (left) and 0.0 (right). **b.** Histogram of vesicularity data from the gray interval in the SCC tephra at site 3. **c.** Histogram of vesicularity data from the gray interval in TM1 at site 1.

CONCLUSIONS

The data are compatible with the hypothesized three-stage eruption history. Specifically, the complexly stratified fall deposits likely resulted from different pyroclast formation and deposition processes associated with three discrete stages of contrasting eruptive phenomena.

The first stage, forming the lower white interval, was explosive eruption of gas-rich magma, which produced a buoyant plume of tephra, ash, and gas. The internal textural and stratification variations, where present, reflect changing eruption dynamics such as a less steady flux and a highly variable eruption column.

The second stage resulted in deposition of the fine, pink-ash intervals and is related to pyroclastic flows. Coignimbrite ash deposition implies that pyroclastic-flow emplacement occupied only a small time window in the overall progression of eruption processes and was largely exclusive of a buoyant eruption plume.

The third eruptive stage, which produced the gray, vesicle-poor ash and lapilli interval, was most likely related to explosive disruption of lava domes or conduit-plugging cryptodomes. These explosions were most likely caused by rapid decompression of highly viscous, partly solidified magma high in the conduit as a consequence of surface dome collapse. This stage of activity may have been intermittent and coeval with a long period of dome growth, as suggested by minor erosional disconformities within gray-interval tephra.

This study illustrates that some fall deposits are not readily characterized as representing a single eruption style in the relatively short span of a single eruption. The Peralta Tuff fall deposits reflect at least three eruption styles – steady or pulsating convective column, pyroclastic-flow emplacement, decompression-driven explosions related to dome collapse – that represent the prolonged history of the entire eruption cycle of a volcano. Although the internal stratigraphy of Peralta Tuff fall deposits are variable at the centimeter to decimeter scale, the common occurrence of the larger-scale tripartite layering implies that the succession of convective column, pyroclastic-flow emplacement, and explosively interrupted dome growth was intrinsic to the rise and eruption of Bearhead Rhyolite magma.

ACKNOWLEDGMENTS

We thank the Caswell Silver Foundation for funding support for this project. Jim Karner assisted with the SEM image analysis. We are grateful for the thoughtful reviews provided by Fraser Goff and Kirt Kempter.

REFERENCES

Alidibirov, M., and Dingwell, D.B., 2000, Three fragmentation mechanisms for highly viscous magma under rapid decompression: Journal of Volcanology and Geothermal Research, v. 100, p. 413-421.

Carey, S., and Sigurdsson, H., 1987, Temporal variations in column height and magma discharge rate during the 79 A.D. eruption of Vesuvius: Geological Society of America Bulletin, v. 99, p. 303-314.

Carey, S., and Sparks, R.S.J., 1986, Quantitative models of the fallout and dispersal of tephra from volcanic eruption columns: Bulletin of Volcanology, v. 48, p. 109-125.

Cas, R.A.F., and Wright, J.V., 1987, Volcanic successions: London, Allen and Unwin Ltd., 528 p.

Ellisor, R., Wolff, J., and Gardner, J.N., 1996, Outline of the petrology and geochemistry of the Keres Group lavas and tuffs: New Mexico Geological Society, 47th Field Conference, Guidebook, p. 237-242.

Folk, R.L., 1974, Petrology of sedimentary rocks: Austin, TX, Hemphill Publishing Company, 182 p.

Gardner, J.N., Goff, F., Garcia, S., and Hagan, R.C., 1986, Stratigraphic relations and lithologic variations in the Jemez volcanic field: Journal of Geophysical Research, v. 91, p. 1763-1778.

Houghton, B.F., and Wilson, C.J.N., 1989, A vesicularity index for pyroclastic deposits: Bulletin of Volcanology, v. 51, p. 451-462.

Justet, L., and Spell, T.L., 2001, Effusive eruptions from a large silicic magma chamber: the Bearhead Rhyolite, Jemez volcanic field, NM: Journal of Volcanology and Geothermal Research, v. 107, p. 241-264.

Klug, C., and Cashman, K.V., 1996, Permeability development in vesiculating magmas: implications for fragmentation: Bulletin of Volcanology, v. 58, p. 87-100.

Lewis, D.W., and McConchie, D., 1994, Analytical sedimentology: New York, Chapman & Hall, 197 p.

Marshall, J.R., and Sheridan, M.F., 1987, Comparative charts for quantitative analysis of grain-textural elements on pyroclasts, *in* Marshall, J.R., ed., Clastic particles: scanning electron microscopy and shape analysis of sedimentary and volcanic clasts: New York, Van Nostrand Reinhold Company, Inc., p. 98-121.

Smith, G.A., 2001, Development of a pyroclastic apron adjacent to rhyolite domes in a subsiding basin: Upper Miocene Peralta Tuff, Jemez Mountains, New Mexico: New Mexico Museum of Natural History and Science, Bulletin 18, p. 85-96.

Smith, R.L., and Bailey, R.A., 1966, The Bandelier Tuff: a study of ash-flow eruption cycles from zoned magma chambers: Bulletin Volcanologique, v. 29, p. 83-104.

Smith, R.L., Bailey, R.A., and Ross, C.S., 1970, Geologic map of the Jemez Mountains, New Mexico: U.S. Geological Survey, Miscellaneous Investigations Map I-571, scale 1:125,000.

Wilson, C.J.N., and Hildreth, W., 1997, The Bishop Tuff: new insights form eruptive stratigraphy: Journal of Geology, v. 105, p. 407-439.